

We are IntechOpen, the world's leading publisher of Open Access books Built by scientists, for scientists

6,400

Open access books available

174,000

International authors and editors

190M

Downloads

Our authors are among the

154

Countries delivered to

TOP 1%

most cited scientists

12.2%

Contributors from top 500 universities



WEB OF SCIENCE™

Selection of our books indexed in the Book Citation Index
in Web of Science™ Core Collection (BKCI)

Interested in publishing with us?
Contact book.department@intechopen.com

Numbers displayed above are based on latest data collected.
For more information visit www.intechopen.com



Chapter

CSF Bypass Surgery in Children with Hydrocephalus: Modern Possibilities, Prospects and Ways of Solving the Correction of Complications

*Konstantin A. Samochernykh, Yulia M. Zabrodsкая,
Mikhail S. Nikolaenko, Olga N. Gaykova, Aleksandr V. Kim,
Elena G. Potemkina, Aleksandr P. Gerasimov,
Nikita K. Samochernykh, Aleksey A. Petukhov,
Eleonora T. Nazaralieva and Wiliam A. Khachatryan*

Abstract

The chapter discusses modern and promising approaches to the use of CSF shunting operations in children. CSF shunting operations remain the only effective method for correcting persistent CSF circulation disorders in CSF resorption disorders with the development of intracranial hypertension and hydrocephalus. The chapter is devoted to general ideas about CSF dynamics and biomechanical properties of the craniospinal system that affect CSF dynamics, and gives a pathogenetic assessment of CSF dynamics in the development of intracranial hypertension and hydrocephalus. Aspects of genetics and genomics of anomalies in hydrocephalus are touched upon. Pathological changes in the brain around old ventricular shunts are described. The authors consider the types of CSF shunting operations for hydrocephalus in children. Possible complications of CSF shunting operations are analyzed with the algorithm for their correction and management tactics for this group of patients.

Keywords: hydrocephalus, intracranial hypertension, craniospinal system, biomechanics, CSF dynamics, CSF bypass surgery, pathomorphology, genetic, complication

1. Introduction

Hydrocephalus has always been and remains one of the most complicated problems of pediatric neurosurgery. The progressive course of hydrocephalus leads to severe neurological and mental disorders with a lag in intellectual and physical

development, significantly affecting the incidence of disability and mortality of the child population.

The term “hydrocephalus” (from others-Greek ύδωρ “water” + κεφαλή “head”), synonymous with “dropsy of the brain,” is an excessive accumulation of cerebrospinal fluid (CSF) in the ventricles of the brain and/or external cerebrospinal spaces, accompanied by their expansion [1].

The problems of hydrocephalus pathogenesis, diagnosis, and treatment have always been relevant at all stages of neurology and neurosurgery development. Hydrocephalus affects an average of five children out of every thousand newborns. In neurosurgical patients, hydrocephalus syndrome is detected in every fourth patient. In one-third of children with hydrocephalus, the development of hydrocephalic hypertension syndrome is one of the causes of decompensation of the patient’s condition [2–4].

Among central nervous system (CNS) injury cases of 25–80% lead to hydrocephalus as a complication at the late stages of the disease, while only 5–10% of cases develop in the acute period. In most patients with pathology of cerebral vessels (mainly ruptured cerebral aneurysms), persistent hydrocephalus, which needs correction, is observed in 5–7% of cases, and it is often found in strokes (up to 60%).

According to the data, the prevalence of congenital hydrocephalus ranges from 2.5 to 8.2 cases per 10,000 newborns, and in patients with malformations of the brain or spinal cord hydrocephalus is observed in up to 78% of cases. In patients with brain tumors, hydrocephalus occurs in 20–94%, with cerebrovascular pathology—in 6–67% of cases, with inflammatory diseases of the CNS—up to 5–60% of cases [5–7], with the indicators increasing every year. The mortality rate in hydrocephalus used to be more than 50% before the valvular fluid bypass operations were introduced. Since these operations became regular practice the mortality rate decreased to 2–5% [8].

State-of-the-art research considers hydrocephalus to be the result of persistent disorders of the CSF circulation.

2. Cerebrospinal fluid circulation and biomechanical properties of the craniospinal system (CSS)

2.1 Cerebrospinal fluid

CSF is normally a pure colorless liquid with a relative density of 1.007 and a pH of ≈ 7.33 –7.35. Basically, it is produced by the vascular plexuses of the lateral, III and IV ventricles, passing through the holes of Monroe, the water supply of the brain, the holes of Mazhandi and Lyushka, and enters the subarachnoid space of the brain and spinal cord, from where it is absorbed into the venous system through a system of channels and pachyonic granulations [9, 10]. Two-thirds of the CSF volume is considered to be of choroidal origin. The other part of CSF is produced by the ependyma of the brain, its membranes, and brain tissue [11].

The rate of CSF production is 0.3–0.5 ml/min and it depends mainly on blood pressure, from the pressure in the choroidal artery, and from the activity of the membrane mechanisms involved in the formation of CSF—to be precise.

CSF absorption occurs through the membranes of the parasagittal zone (arachnoid granulations) of the brain. This is how the resorption of the main volume (2/3) of CSF is carried out. The other part of the CSF is absorbed through the membranes of the meningeal sheaths of spinal and cranial nerves, membranes, and parenchyma of the

brain. Under normal conditions, the rate of CSF resorption is balanced with its production [5, 10, 11].

2.2 Structural units of the cerebrospinal fluid circulation system

The ways of CSF circulation are fairly well described. The CSF circulates in a certain direction. Under normal conditions, CSF from the lateral ventricles through the holes of Monroe enters the III ventricle, then into the water supply of the brain and the IV ventricle. Further, through the holes of Luschka and Magendie, CSF enters the cisterns of the base of the brain (cerebellar-cerebral, covering the cistern of the bridge, chiasm, and the cistern of the Sylvian furrow) and then onto the convexity surface into the subarachnoid space. Channels and cells of arachnoid shells are structural units of the liquor outflow pathway system. However, in pathological conditions, the arachnoid shell, being highly reactive, is able to rapidly proliferate arachnoid cells with the walls thickening, to accumulate water by collagen fibers, which finally disrupts normal circulation of the CSF.

Part of the CSF from the spanning cistern of the bridge enters the cisterns of the cerebellar worm. A smaller volume part of the CSF enters the cerebrospinal subarachnoid space (**Figure 1**).

The volume of the cranial part of the CSF is about 68% of the total volume of the craniospinal cavity, and the spinal part is 32%, respectively. Approximately 1/3 of the CSF volume is located in the ventricles of the brain, 1/3—in the subarachnoid cerebral and 1/3 of the volume—in the spinal subarachnoid spaces [4, 5, 10–12].

2.3 Physiological support of CSF circulation

CSF outflow is provided by the presence of a pressure gradient (15–30 mm of water) between the ventricles of the brain and the subarachnoid space [9].

CSF absorption is achieved due to the difference in pressure in the brain sinuses and CSF pressure. The rate of CSF resorption is directly proportional to the amount of CSF pressure and inversely proportional to the venous pressure in the upper

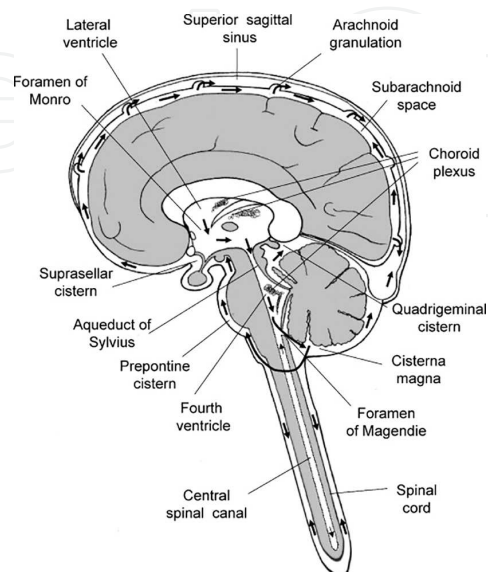


Figure 1.
Scheme of structural units and pathways of cerebrospinal fluid circulation [5].

longitudinal sinus [5, 9]. The intracranial pressure remains relatively stable, and with an increase in intracranial pressure up to 300 mm of water column CSF resorption becomes inhibited. The pressure in the upper sagittal sinus is about 12 mm Hg. With the CSF and intrasinus pressures being equalized (below 5 mm Hg), CSF resorption is disrupted. With an increase in intracranial pressure greater than 7 mm of water column, a linear increase in the rate of CSF resorption is observed [13, 14].

Resorption resistance is a characteristic reflecting the state of the CSF pathways and CSF outflow pathways into the venous system. Due to the fact that the resorption rate is linearly dependent on the pressure gradient, a change in the resorption resistance of the CSF is of practical importance [9, 11].

Pulse fluctuations have a significant effect on the CSF circulation, the volume of blood in the cranial cavity, and the waves propagate in the caudal direction.

Respiratory wave fluctuations in liquor pressure caused by the formation of respiratory pressure waves in the pleural and abdominal cavities are transmitted to the veins in the cavities of the skull and spine. Respiratory waves of venous pressure cause the flow of CSF from the cranial to the spinal cavity. Respiratory waves of arterial pressure and pressure in the inferior vena cava normally do not affect the fluctuation of intracranial pressure.

The liquor pressure equal to 112–130 mm of water column (about 9–10 mm Hg) is theoretically a “normal” pressure [5, 10, 11]. Normally, at constant pressure in the craniospinal cavity, the amount of liquor produced is equal to the volume of the absorbed.

The reasons for the excessive accumulation of CSF can be:

- acceleration of production,
- deceleration of suction,
- violation of transport through the liquor-diverting ways.

Excessive accumulation of CSF leads to a violation of the dynamic equilibrium of “production-resorption” and to the expansion of the cerebrospinal cavities and the decrease in the volume of the medulla [11, 15, 16].

2.4 Volumetric components of CSS

The “Monro-Kellie” theory describes the volumetric relationships within the CSF, or craniospinal cavity. The up-to-date version of the theory asserts that three volumetric components capable of changing their quantitative values are determined in the relatively rigid cavities of the skull and spine [5]:

1. Brain tissue with membranes.
2. Vascular bed with circulating blood.
3. Liquor system with CSF constantly formed and absorbed in it

The craniospinal cavity is represented by a closed space, limited by the meninges, in which the brain and spinal cord are enclosed. Some elasticity of the formations of the cranial cavities was also noticed due to the malleability of the tissues of the atlanto-

occipital membrane, the multitude of holes at the base of the skull, as well as the possibility of divergence of sutures in children with intracranial hypertension (ICH). Spinal tissues have significantly greater elasticity due to the extensibility of the intervertebral ligaments and the possibility of protrusion of the dura mater at the exit points of the spinal nerves. With the development of the pathological process at the compensation stage, an increase in one of these volumes is accompanied by a change in the other.

CSS has the properties of elastic materials of malleability (elasticity), viscosity (fluidity) and can be expressed mathematically [5, 10, 11, 17].

The malleability of brain tissue is characterized by the ability to deform under mechanical action. Malleability is closely related to the extensibility of interstitial spaces. The viscoelastic characteristics of the CSS vary depending on the inner pressure.

The biomechanical properties of CSF consist of the malleability of the bones of the cranial vault, the connective tissue membranes of the spine, the state of CSF circulation, changes in blood volume, and the degree of accumulation of water by the brain tissue. The malleability of the entire CSF is an algebraic sum of these indicators for the cranial and spinal cavities [5, 9, 11].

Blood volume and blood pressure level play an important role in changing the elasticity of the CSF. An increase in blood pressure leads to an increase in the volume of the brain due to an increase in the volume of blood in its vessels, an increase in the volume of water filtration, and an increase in the volume of the brain tissue itself, which occurs with a sharp increase in systolic blood pressure, when compensatory constriction of the arteries does not have enough time to develop in response to the increase in blood flow. Unlike arterial pressure, an increase in the venous pressure of the brain immediately leads to the directly proportional increase in intracranial pressure [11].

2.5 Quantitative indicators of liquor circulation and viscoelastic properties of CSF

Liquor circulation has a significant effect on the mechanical properties of CSF. The change of individual links of the liquor circulation is aimed at maintaining the constancy of the value of the resulting characteristic—the liquor pressure. Disruption of the compensatory capabilities of the CSS is manifested in the development of cerebrospinal hypertension.

Quantitative indicators of CSF circulation and viscoelastic properties of CSF are studied by the method of artificial change of CSF volume and registration of pressure changes in the craniospinal cavity [10, 15, 18].

Two reciprocal curves are used for quantitative characterization: “pressure–volume” P/V , characterized by an “exponential” dependence, or “volume–pressure” V/P (inverse P/V dependence). Both curves display the viscoelastic properties of the CSS and have three characteristic sections (**Figure 2, A, B**).

The fragment of the curve (a-b) has a flat section, as well as a section of a sharp increase in pressure (c-d) and an intermediate period (b-c). These sections of the curve correspond to the state of the system’s backup capabilities. In other words, the elasticity of the system increases exponentially with the development of ICH.

There are three phases in ICH the system goes through: compensation, sub-, and decompensation. In the phase of compensated ICH (site a–b), there is a moderate increase in intracranial pressure, a slight increase in the elasticity gradient, a decrease in malleability, a normal value of resorption resistance, and the rate of CSF production.

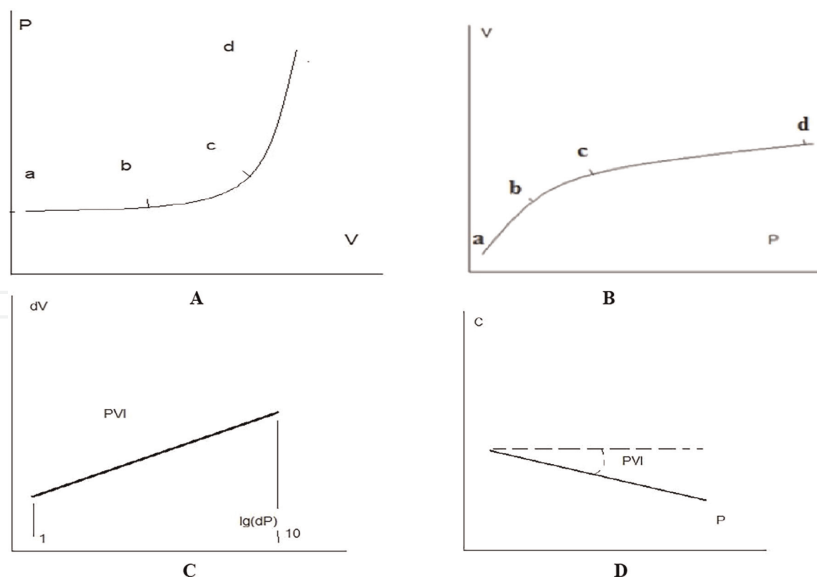


Figure 2. Viscoelastic properties of SCC. A—*P/V-dependence graph*; B—*V/P-dependence graph*; C—*logarithmic indicator of P/V dependence (pressure-volume index, PVI)*; D—*CSS compliance*. *P*—*liquor pressure*, *V*—*liquor volume*, *C*—*compliance CSS*.

In the subcompensation phase (b–c), there is an increase in intracranial pressure and an increase in resorption resistance. The decompensation phase (c–d) is characterized by the exhaustion of reserve mechanisms, increasing intracranial pressure, decreased CSF production, increased resorption resistance, and elasticity [5, 10, 11].

Marmarou A. and co-authors (1975) proposed a characteristic of the elastic properties of the system—the “pressure-volume” index (Eq. (1)).

$$PVI = \frac{dV}{\lg\left(\frac{P_p}{P_0}\right)} \text{ (ml)} \quad (1)$$

where:

- PVI*—index “pressure-volume”,
- dV*—volume change of the CSS,
- P_p*—increased liquor pressure after bolus administration,
- P₀*—initial liquor pressure before the bolus.

They processed the obtained data of the pressure-volume relationship using the logarithmic method and obtained a linear relationship [5] (**Figure 2, C**).

A linear equation for determining the compliance of the CSS was also proposed (**Figure 2, D**).

$$C = 0,4343 \cdot \frac{PVI}{P} \text{ (ml/mm of water)} \quad (2)$$

where:

- C*—compliance (compliance),
- P*—the liquor pressure at a given time.

The angle of inclination of the curve is an individual constant characteristic of each individual CSS and reflects its compliance, individual ability to maintain constant

parameters during the development of any volumetric process (Eq. (2)). The pressure-volume index is a constant characteristic of the system in the compensation stage. Compliance is a dynamic characteristic of the system; it inversely depends on intracranial pressure [5, 11].

Pliability, elasticity of the CSS are individual characteristics. As the compensation mechanisms of the system are depleted in conditions of growing ICH, the elasticity of the CSF increases. According to various authors, normal PVI values are considered to be more than 25 ml. PVI indicators in children range from 8.2 to 30.1 ml [9, 10].

Thus, the viscoelastic properties of the craniospinal cavity are due to:

- its anatomical dimensions,
- the state of stretchable formations,
- biomechanical properties of the actual brain tissue,
- the state of the liquor circulation system,
- the state of the venous outflow of blood from the cranial cavity,
- changes in arterial blood filling.

3. Pathomorphology of hydrocephalus

Occlusive hydrocephalus is the most common among all types of hydrocephalus. It develops in early childhood and is associated with malformations of the CNS, the consequences of birth trauma, or intrauterine infection, accompanied by occlusion of the Lyushka holes and Majandi spikes.

In the first months of life the child's head circumference increases rapidly (sometimes up to 2 cm per week), reaching 50–100 cm by the age of 12 months. At the same time, the bones of the skull become thinner, the cranial sutures diverge, the bone structures of the Turkish saddle atrophy, and the pituitary gland is usually somewhat reduced in size and compressed (flattened). The ventricles of the brain are expanded to one degree or another, the brain cloak gradually atrophies, and its thickness can decrease to 5 mm. The brain in this case is a bubble filled with CSF. A child suffering from severe hydrocephalus is practically deprived of both coordinating systems—nervous and endocrine ones. Such patients can suddenly die from pain or emotional stress, mild acute respiratory viral diseases, etc. Without treatment they die, as a rule, at the age of two years.

4. Genetics and genomics of anomalies in hydrocephalus

Abnormalities of CNS are multifactorial. Both genetic and external factors may be critical, and they may be presented in the combination with synergy effect.

As of today, several groups of genes, associated with CNS abnormalities, are described. Methods of system genomics proved very useful for understanding

neuropathology development [19]. Our analysis was based on OMIM database actual at 17.01.23.

The most catastrophic scenario is neural tube defect up to hydroanencephaly. Combination of genetic and environmental factors is well described in Ref. [20]. Group of genes, associated with susceptibility to neural tube defects (182940), is presented in **Table 1**.

VANGL1 and VANGL2 are very similar with 73.1% primary amino acid sequences identity. Clinical cases are described both in family and sporadic forms [21]. All the forms in this group are autosomal dominant.

Errors in the folic acid cycle may cause neural tube defects. Group of folate-sensitive neural tube defects (NTDFS) (601634) is presented in **Table 2**.

Variants in MTHFR, MTR, MTRR, and MTHFD1 may lead to change in folic acid and cysteine concentration. Moreover, they may change individual need in folic acid and cobalamin. Clinical aspects are well described in [22].

Three autosomal recessive forms of congenital hydrocephalus are described (**Table 3**).

Additionally, 3 clinical variants (307000) with X-linked recessive inheritance are associated with L1CAM gene. Typical mechanism observed in this case is congenital stenosis of the aqueduct of Sylvius [23].

Megalencephaly-polymicrogyria-polydactyly-hydrocephalus syndrome (MPPH) is caused by heterozygous mutation in 3 genes. This fact illustrates genetic heterogeneity of clinically similar states [24] (**Table 4**).

Several forms of genetic hydrocephalus in combination with other clinical features are described, usually as clinical cases. Generally, mutations in different genes may

Location	Phenotype	Phenotype MIM number	Inheritance	Gene/Locus	Gene/Locus MIM number
1p13.1	{Neural tube defects, susceptibility to}	182,940	AD	<i>VANGL1</i>	610,132
1q23.2	Neural tube defects	182,940	AD	<i>VANGL2</i>	600,533
6q27	{Neural tube defects, susceptibility to}	182,940	AD	<i>TBXT</i>	601,397
17q12	{Spina bifida, susceptibility to}	182,940	AD	<i>CCL2</i>	158,105
19q13.33	{Neural tube defects, susceptibility to}	182,940	AD	<i>FUZ</i>	610,622

Table 1.
Susceptibility to neural tube defects.

Location	Phenotype	Phenotype MIM number	Inheritance	Gene/Locus	Gene/Locus MIM number
1p36.22	{Neural tube defects, susceptibility to}	601,634	AR	<i>MTHFR</i>	607,093
1q43	{Neural tube defects, folate-sensitive, Susceptibility to}	601,634	AR	<i>MTR</i>	156,570
5p15.31	{Neural tube defects, folate-sensitive, susceptibility to}	601,634	AR	<i>MTRR</i>	602,568
14q23.3	{Neural tube defects, folate-sensitive, susceptibility to}	601,634	AR	<i>MTHFD1</i>	172,460

Table 2.
Folate-sensitive neural tube defects.

Location	Phenotype	Inheritance	Phenotype MIM number	Gene/Locus	Gene/Locus MIM number
14q32.11-q32.12	Hydrocephalus, congenital, 1	AR	236,600	CCDC88C	611,204
9p23	Hydrocephalus, congenital, 2, with or without brain or eye anomalies	AR	615,219	MPDZ	603,785
17p13.3	Hydrocephalus, congenital, 3, with brain anomalies	AR	617,967	WDR81	614,218
Xq28	Hydrocephalus due to aqueductal stenosis	XLR	307,000	L1CAM	308,840
Xq28	Hydrocephalus with Hirschsprung disease	XLR	307,000	L1CAM	308,840
Xq28	Hydrocephalus with congenital idiopathic intestinal pseudoobstruction	XLR	307,000	L1CAM	308,840

Table 3.
Congenital hydrocephalus.

Location	Phenotype	Inheritance	Phenotype MIM number	Gene/Locus	Gene/Locus MIM number
19p13.11	Megalencephaly-polymicrogyria-polydactyly-hydrocephalus syndrome 1	AD	603,387	PIK3R2	603,157
1q43-q44	Megalencephaly-polymicrogyria-polydactyly-hydrocephalus syndrome 2	AD	615,937	AKT3	611,223
12p13.32	Megalencephaly-polymicrogyria-polydactyly-hydrocephalus syndrome 3	AD	615,938	CCND2	123,833

Table 4.
Megalencephaly-polymicrogyria-polydactyly-hydrocephalus syndrome.

cause similar phenotypes, and mutations in one gene may lead to different clinical variants. Many pathways may be discussed, but the two are evident: errors in folic acid exchange and genetic-related stenosis of the aqueduct of Sylvius.

5. Assessment of intracranial hypertension and hydrocephalus syndrome

5.1 CSF infusion test or infusion-load test (ILT)

ILT with the calculation of resorption resistance of the CSF was one of the fundamental methods in choosing of surgical treatment of patients with hydrocephalus [9].

During ILT, the bolus infusion technique of A. Marmarou is used. To do this, a ventricular catheter is inserted into the cavity of the lateral ventricle. The distal

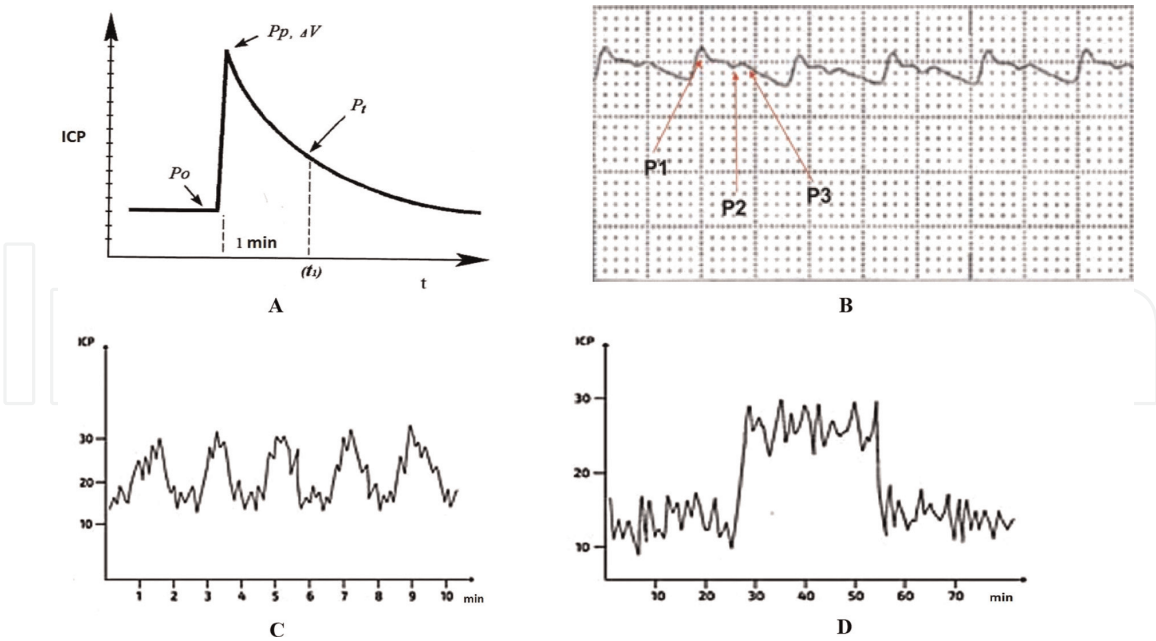


Figure 3.
 A—Bolus INT circuit with recorded parameters: P_o —initial liquor pressure; P_p —maximum pressure after bolus injection. P_t —liquor pressure after bolus injection after 1 minute in the relaxation phase; ΔV —volume of injected fluid. B is the type of pulse wave of ICP with a compensated state of intracranial compliance. P_1 —Systolic peak, P_2 —Vascular peak, P_3 —Diastolic peak. C—pathological Lundberg waves of type B caused by an increase in ICP without depletion of intracranial compliance. D—pathological Lundberg waves of type A caused by increased ICP with depletion of intracranial compliance.

part of the ventricular catheter is connected to the ILT system. Within 2 minutes the background intracranial pressure, background spectral components of wave oscillations are recorded. Next, a saline solution is injected with a bolus volume of 2 ml at a rate of 1 ml/sec with an interval between boluses of 1 min [4, 10, 15, 17] (**Figure 3, A**).

From the ratio of the injected volume, the magnitude of the maximum increase in pressure and pressure after 1 minute during the relaxation period, according to A. Marmarou's formula, both the production rate (A) and the resorption resistance index (R) (a value proportional to the inverse value of its absorption) are calculated using an infusion-liquor test, which is based on excretion and administering a certain volume of CSF by boluses or once and measurement of the time during which the cerebrospinal pressure is restored as a result of CSF production or suction [15, 25].

The calculation is carried out according to the formulas:

1. CSF production rate (A) (Eqs. (3) and (4)):

$$\frac{\Delta V_1 \cdot \lg\left(\frac{P_1}{P_m}\right)}{t_1 \cdot \lg\left(\frac{P_0}{P_m}\right)} \quad (3)$$

2. CSF resorption resistance (R) (Eq. (4)):

$$\Delta V_2 \cdot \lg \left[\frac{P_2 \cdot (P_p - P_0)}{P_p \cdot (P_2 - P_0)} \right] \quad (4)$$

- V1 is the volume of the withdrawn liquid, P0 is the initial liquor pressure, Pm is the pressure immediately after the evacuation of the bolus, P1 is the pressure after a certain time t1,
- V2 is the volume of the injected liquid, Pp is the maximum pressure after injection, and P2 is the pressure on the curve of the reduction of the liquor pressure after injection after a certain period of time t2.

The evaluation of ILT results consists in the determination of intracranial pressure, fluctuations of CSF (amplitude-frequency changes), as well as registration of resorption resistance of CSF, followed by obtaining one of the variants of pressure-volume curves (P/V): normotensive, hypertensive, and atrophic [15].

5.2 Monitoring biomechanical properties of CSS in case of ICH

Currently, discrete values of intracranial pressure are of low practical importance, since they do not display indicators of intracranial compliance (ICC). To assess the severity of the pathological process in patients with increased ICP of various etiologies, including hydrocephalus and congenital malformations of the skull bones, an assessment of the pulse curve recorded when measuring ICP is used. These changes are typical of ICC changes of any etiology and characterize the amplitude of pulse oscillations, the morphology of pulse curve peaks, and the formation of plateau waves with a significant decrease in compliance. The classical view of the pulse curve is shown in **Figure 3, B**.

One cardiac cycle forms three peaks due to the increase in intracranial volume in the systole and its decrease in the diastole.

Accordingly, the P1 (systolic) peak turns out the most pronounced one on the normal ICP curve. Immediately upon reaching the pulse wave of the microcirculatory bed of the brain, a P2 peak should appear as the reaction of the arterial bed muscular layer to compensate systolic pressure and normalize the curve, and reduce the amplitude of pulse oscillations. At the moment of diastole, a dicrotic P3 peak is formed, which characterizes a decrease in intracranial blood volume and relaxation of the vascular bed. The morphology of the pulse curve depends on the initial state of the ICC and the volume of increase in the intracranial contents, which manifests clearly and underlies the infusion-load testing.

Formulas were used for discrete assessment of biomechanical properties and liquor circulation [15]:

$$PVI_d = \frac{dV_b}{\lg \left(\frac{\text{meanICP}_p}{\text{meanICP}_o} \right)} \quad (5)$$

where PVI_d is the discrete value of the PVI index; meapISR_o is the average liquor pressure before bolus administration; mean ICP_p is the average liquor pressure after bolus administration; dV_b is injected (with a plus sign)/output volume (with a minus sign) of the bolus, ml.

$$C_d = \frac{0,4343 \cdot PVI_d}{meanICP_o} \quad (6)$$

where C_d is a discrete assessment of craniospinal compliance.

$$I_d = \frac{PVI_d \lg \left[\frac{(meanICP_p)}{(meanICP_t)} \right]}{dT} \quad (7)$$

where I_d is a discrete estimate of the rate of resorption/production of CSF; dT is the time interval in minutes from the moment of bolus injection/withdrawal to the current meanICPt average pressure.

$$R_d = \frac{dT \cdot meanICP_o}{PVI_d \lg \left[\frac{meanICP_t (meanICP_p - meanICP_o)}{(meanICP_t - meanICP_o) meanICP_p} \right]} \quad (8)$$

where R_d is a discrete estimate of the resorption resistance of the CSF.

In addition to changes in the pulse curve, the classic signs of an increase in ICP and a decrease in ICC are the appearance of pathological plateau waves (Lundberg waves) on the ICP monitoring chart. There are three types of waves—A, B, C—while only type B and C waves are indicative of this or that change in compliance. Type C waves are associated with respiratory and cardiac cycles, manifested by an increase in ICP of a small amplitude. Their duration does not exceed the specified cycles. Type B waves are manifested by an increase in ICP to 30–50 mmHg and a duration of 1–5 minutes (**Figure 3, C**). Most often, the appearance of these waves is considered to provoke ICC without its obvious depletion. The appearance of type A waves—prolonged, up to 40 minutes, persistent increases in ICP up to 50 mmHg and above—is associated with the depletion of ICC (**Figure 3, D**).

The universality of these parameters resulting from compliance changes of any etiology seems to be significant. The identification of the ICP increase plateau is a significant diagnostic criterion for “latent” ICH, which is most often encountered in the long course of the pathological process. HCG in hydrocephalus can serve as an example of such condition, developing in patients with congenital malformations of the skull bones, or in patients with subcompensated forms of hydrocephalus in the neonatal period, when classical clinical signs of ICH are extremely rare.

5.3 Imaging methods, indices of the ventricular system of the brain

Modern imaging methods make it possible to identify hydrocephalus, establish the cause of the development of this process, conduct dynamic observation, and evaluate the effectiveness of the performed liquor bypass surgery. Currently, magnetic spiral computed tomography (MSCT) is considered to be the optimal method of radiation diagnosis of hydrocephalus, the use of which allows you to quickly measure the size and count the indices of the ventricular system of the brain, which is especially important in childhood when planning surgical treatment [26, 27].

When interpreting the conducted radiation examination, the symmetry, degree of expansion, configuration, and contours of the ventricular system are taken into account.

The index of the anterior horns of the lateral ventricles is calculated in relation to the maximum distance between the most distant external parts of the anterior horns and the maximum bitemporal diameter of the skull multiplied by 100. Normally, the value of this index ranges from 25.4 (under the age of 5 years) to 29.4–31.0 (aged 71 to 80 years) (**Figure 4, A**).

The index of the central sections of the lateral ventricles is calculated with respect to the smallest distance between their outer walls in the recess area and the maximum bitemporal diameter of the skull on the same slice multiplied by 100. Normally, the value of this index ranges from 18.2 to 26.0 (**Figure 4, B**).

The index of the III ventricle is estimated in relation to its maximum width in the posterior third at the level of the pineal gland to the largest transverse diameter of the skull on the same section, multiplied by 100. Normally, the value of this index increases with age, reaching 3.0 at the age of 5 years and 4.8—from 71 to 80 years (**Figure 4, C**).

The index of the IV ventricle is calculated in relation to its largest width to the maximum internal diameter of the posterior fossa of the skull on the same slice. Normal indicators of this index are 11.9–14.0 (**Figure 4, D**).

Intraventricular hypertension is characterized by the appearance of periventricular edema, there are four stages of these changes:

Stage 1—blurring of the contours of the upper-outer corners of the anterior horns or a clearly limited border of reduced density of the same localization;

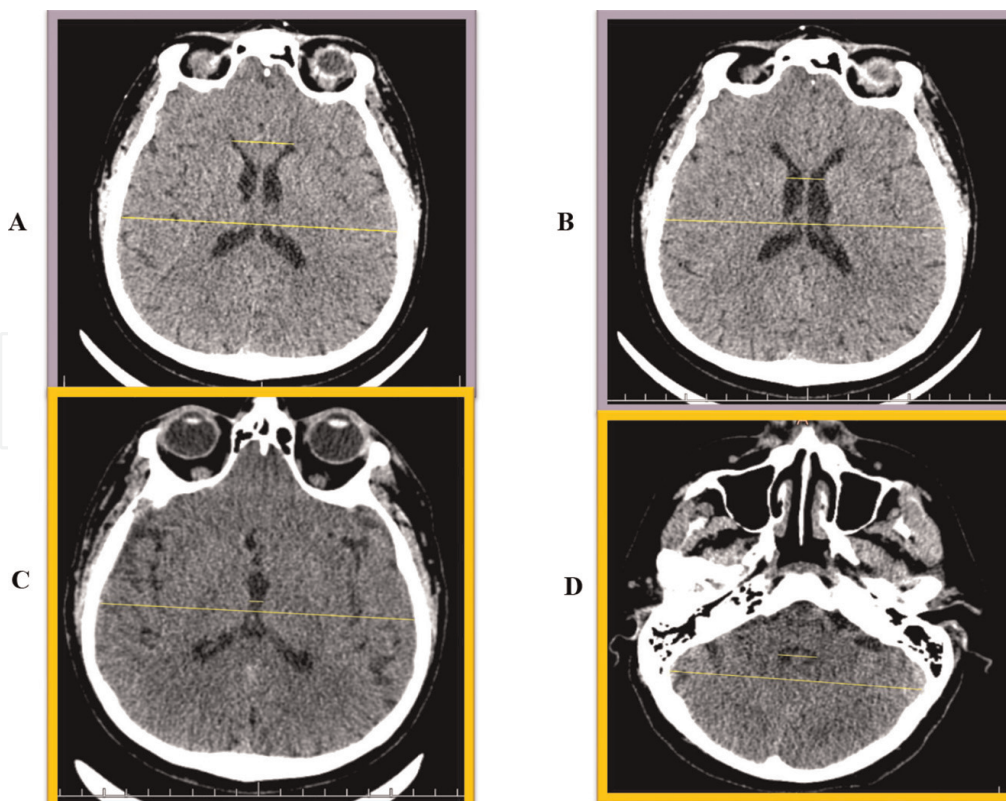


Figure 4. MSCT of the brain. Measurement for calculating the index of the anterior horns of the lateral ventricles (A), measurements for calculating the index of the central divisions of the lateral ventricles (B). Measurement for calculating the index of the III ventricle (C), measurements for calculating the index of the IV ventricle (D).

Stage 2—reduction of density in the anterior and posterior horns;

Stage 3—edema along the perimeter of the lateral ventricles;

Stage 4—scalloped contours of the lateral ventricles and thinning of the brain substance.

Conducting magnetic resonance imaging (MRI) or MSCT with ventriculometry, in combination with a CSF examination, allows to timely diagnose hydrocephalus, to determine the severity and evaluate the results of the treatment.

6. Liquor shunting operations (LSO)

To correct persistent disorders of CSF circulation when it is impossible to use etiotropic treatment of decompensated hydrocephalus, LSO are used. The CSF shunting system is known to be an artificial analogue designed to compensate for disorders of CSF circulation, while its adequate functioning is determined by individual biomechanical parameters of the CSS.

Clinical and neuroimaging criteria, as well as their relationship with quantitative indicators of cerebrovascular circulation and cerebrovascular conjugation, determine the effectiveness of surgical treatment of hydrocephalus in children. Their importance while planning neurosurgical intervention is often underestimated. Solving these important tasks involves studying the disease aspects and taking into account how individual characteristics of the patient manifest—to develop a pathogenetically sound diagnostic system and personalize the hydrocephalus surgical treatment tactics.

In this regard, it is relevant to objectively evaluate these indicators and develop a system of minimally invasive monitoring of the viscoelastic properties of the CSS within the preoperative planning structure and to assess the effectiveness of hydrocephalus surgical treatment, taking into account changes in fluid dynamics.

Liquor anastomosis can be performed using shunts of various systems. The proximal part of the shunt is located in the cavity of the lateral ventricle, then the catheter passes through the brain substance, the soft and hard meninges, and bone and is connected to the pump. The pump is fixed to the bones of the skull and located directly under the skin. The pump valve regulates the pressure of the CSF at a predetermined level and allows it to pass in one direction only—from the cranial cavity to the extracerebral cavities. The distal part of the shunt is attached to the pump; it passes under the skin in the soft tissues of the neck and then, depending on the type of bypass surgery, plunges into the right atrium, transverse sinus, abdominal, pleural cavities, etc. (**Figure 5**).

Treatment of children with hydrocephalus involves various LSO. The removal of the CSF is carried out using implantable valve systems into the peritoneal cavity, with the inexpediency of classical methods, extracranial removal of CSF into the bloodstream (right atrium, jugular vein, sinuses of the dura mater, etc.) is used [28].

Indications for the CSF shunting operations with permanently implanted valve systems are persistent violations of CSF resorption, limiting the ability to normalize CSF circulation within the CSF system;

When choosing the parameters of the throughput of the CSF shunting system, they proceed from the results of measuring the biomechanical properties of the CSS and CSF circulation during surgery.

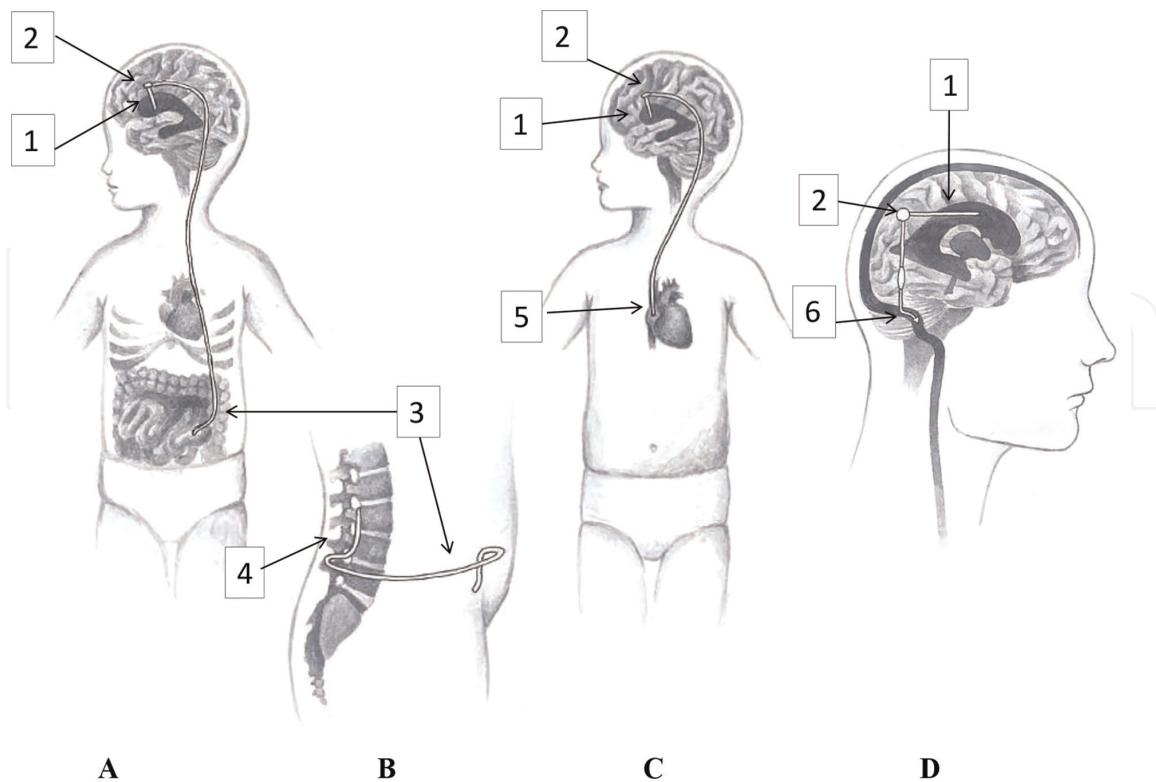


Figure 5. Types of CSF bypass surgery. A—Scheme of ventriculoperitoneostomy. B—Scheme of lumboperitoneostomy. C—Scheme of ventriculoatriostomy. D—Scheme of ventriculosinuostomy. 1—Ventricular catheter; 2—Bypass system valve; 3—Peritoneal catheter; 4—Lumbar catheter; 5—Atrial catheter; 6—Sinus catheter.

Types of LSO:

- **Ventriculoperitoneostomy (Figure 5, A).** During this operation, an anastomosis is formed between the ventricle of the brain and the abdominal cavity [10, 29].
- **Lumboperitoneostomy (Figure 5, B).** During this operation, an anastomosis is created between the CSF-containing space of the spinal canal and the abdominal cavity (mainly with the communicating form of decompensated hydrocephalus). Puncture lumboperitoneostomy is relatively low-traumatic; therefore, as of today, this operation is considered to be preferable in communicating hydrocephalus treatment [10, 15].
- **Ventriculoatriostomy (Figure 5, C).** During ventriculoatriostomy, an excessive amount of CSF from the ventricular system is removed into the right atrium cavity [10].
- **Ventriculosinuostomy (Figure 5, D).** Unlike ventriculoperitoneostomy and ventriculoatriostomy, a distal catheter is implanted into one of the transverse sinuses. For ventriculosinuostomy, a low or very low pressure drainage system is used. Bilateral ventriculosinuostomy is not performed [12].

7. Pathomorphological changes of the brain around long-standing ventricular shunts

The puncture canal is a model of minor surgical brain damage and its outcome. Prolonged presence of an inert foreign body (shunt) determines the features of changes in the surrounding brain tissue [30].

As shown by a postmortem examination of brain tissue around shunts installed in occlusive hydrocephalus with various pathologies, a structured gliomesodermal capsule is formed more than 20 days ago (Figure 6).

As a result of completed reparative processes after puncture damage, along with a capsule mainly formed by mast astrocytes with connective tissue elements, a zone of perifocal changes in brain matter is detected, manifested by damage to myelin fibers and microcystic transformation (Figure 7).

Despite minimal brain damage during puncture, the outcome of reparative processes around the canal is the formation of a functionally “mute” zone, which is recorded during MRI examination in the form of a hyperintensive signal on T2 VI, IR IP, extending from the wall of the puncture canal up to 3 cm. The observed severity of perifocal changes around the shunt may cause neurological manifestations.

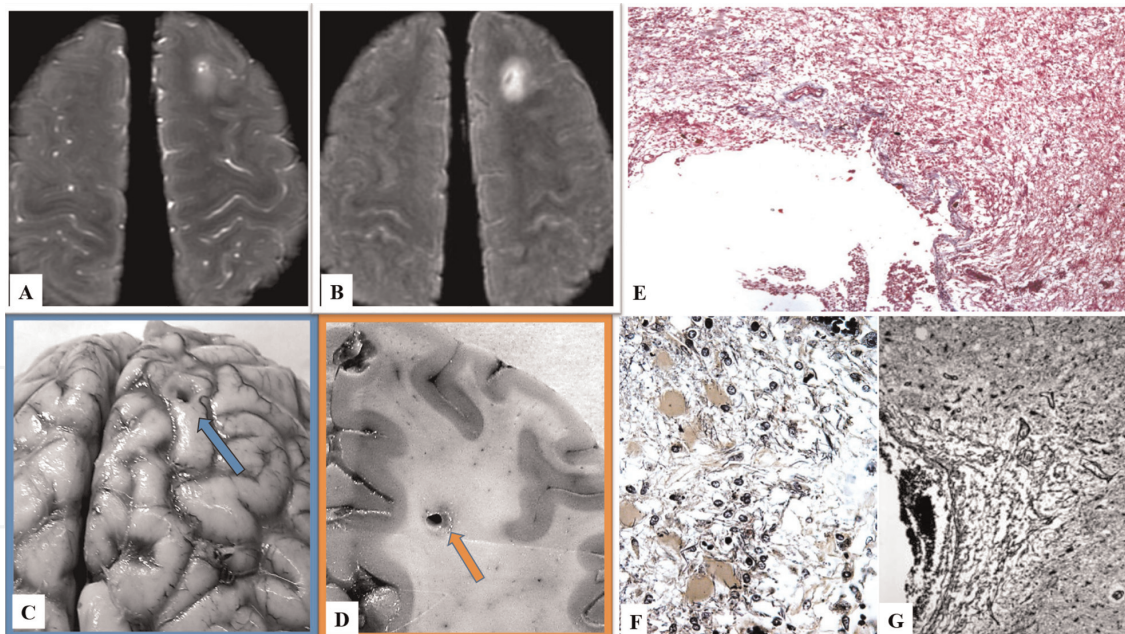


Figure 6.

Puncture canal in the right frontal lobe after installing a ventriculoperitoneal shunt through the anterior horn of the right lateral ventricle. The limitation period is 30 days. A—MRI T2-VI, axial plane. The three-layer structure of the puncture canal zone is differentiated; B—MRI IP-IR, axial plane. Puncture canal in the form of an oval hypointensive focus surrounded by a zone of perifocal changes; C—anatomical preparation, a type of puncture canal from the convexal surface; D is an anatomical preparation, a horizontal section at the level of the corresponding MR image. Perifocal changes recorded on MRI are not visualized; E—along the edge of the puncture canal is a gliomesodermal capsule with the presence of coarse collagen fibers of connective tissue. X 50. Mallory coloring; F—loose granulation tissue with an abundance of thin-walled vessels and reticulin fibers. X100. Impregnation with silver; G—cell gliosis of fibrous and obese astrocytes, around fragments of myelin fibers. X400. Coloring by Shpilmeyer.

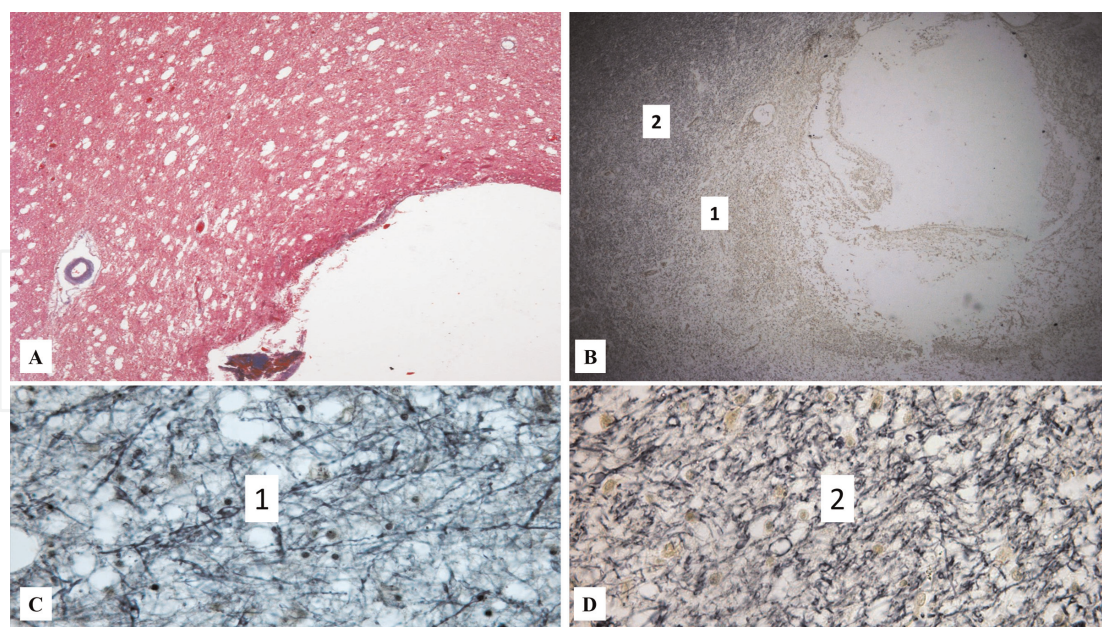


Figure 7. Perifocal changes of the brain around the puncture canal. A—microcystic transformation of brain matter. X 50 H&E; B—demyelination of white matter around the channel. X 50, Shpilmeyer painting; C—single thinned myelin fibers with bulbous thickenings in the demyelination zone. X 200, Shpilmeyer coloring; D—fragmentation and formation of ring-shaped structures of damaged myelin fibers. X 200, Shpilmeyer coloring.

8. Complications of LSO and their correction

The purpose of CSF shunting operations using valve drainage systems is to remove “excess” CSF outside the CSF system, eliminate ICH, and reduce the severity of deformation and expansion of CSF cavities [31].

In some cases, the goal is not achieved, and, with a liquor-shunting system implanted certain pathological manifestations occur. They are mainly associated with the peculiarities of the CSF shunting system functioning, namely with its permanent or transient dysfunction, and are combined into a single group of complications associated with inadequate operation of the shunting system [13, 31–33].

Pathological conditions, which are based on inadequate intensity of CSF outflow, are divided into two large groups: hyperdrainage and hypodrainage complications.

8.1 Hypodrainage conditions

In cases when the CSF outflow through the shunting system is insufficient to balance the CSF circulation and eliminate craniocerebral disproportion, manifestations of decompensated hydrocephalus persist even after CSF shunting operations [33].

This complication manifests in headaches, lethargy, drowsiness, hypophasia, hypodynamia, convergence disorders, paresis of looking up, suppression of photoreactions, suppression of abdominal reflexes, less often paroxysmal manifestations, the occurrence or preservation of pathological stop signs, and oral reflexes are observed. Ophthalmological studies reveal the persistence or reappearance of stagnant phenomena on the fundus, deterioration of vision, the field of vision narrowing.

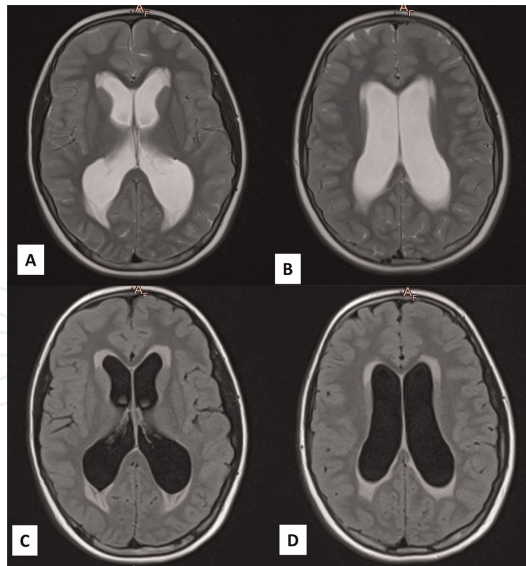


Figure 8. MRI scan, axial projection of the brain 2 months after CSF bypass surgery. Progressive hydrocephalus. Shunt dysfunction. Ventriculomegaly with periventricular edema, absence of subarachnoid spaces. T2WI (A, B), Flair IP (C, D).

More often, a hypodrainage condition is detected during implantation of a drainage system of high or very high (≥ 120 mm of water) pressure, after previously performed ventriculoperitoneostomy or lumboperitoneostomy in patients with previous operations in the abdominal cavity or in the presence of pathology of the abdominal organs. Usually (in 3/4 of patients) hypodrainage is manifested during the first week (month) after surgery, and the progressive course is slow.

CT, MRI studies reveal ventriculomegaly, narrowing of subarachnoid slits, preservation of periventricular edema (**Figure 8**).

The pathogenesis of hypodrainage conditions is far from being understood uniformly. Incorrectly chosen valve parameters of implantable systems can result in the valve pressure being higher than required. As a result, excessive CSF pressure persists. High peripheral resistance resulting from high intra-abdominal pressure, or high central venous pressure in those areas where liquor shunting systems are implanted, is considered to be another reason. There is still another mechanism leading to a hypodrainage state, which is a change in the “pressure-velocity” parameters of implantable systems under *in vivo* conditions due to obliteration of catheters and changes in the patency of the valve system [25, 33–35].

To diagnose a hypodrainage complication, one should state clinical and introsopic manifestations: the persistence of decompensated hydrocephalus, as well as ventriculomegaly, obliteration of subarachnoid spaces, periventricular edema according to CT, and MRI [33].

8.2 Hyperdrainage complications

With inadequately selected parameters of the shunting system, patients with hydrocephalus may develop specific conditions in the postoperative period, which include, inter alia, hyperdrainage complications. These conditions are based on excessively intense CSF outflow through the CSF shunting system, leading to low CSF pressure, accompanied by deformation of the CSF cavities of the brain, skull, and various clinical manifestations [33].

The frequency of this complication is noted in a wide range: from 5 to 55% [31, 35] and is more often observed in children under 6 months. Hyperdrainage leads to the development of such manifestations of craniocerebral disproportion as intracranial hypotension, slit-like lateral ventricle syndrome, subdural accumulation of CSF, isolated IV ventricle syndrome, and other cranial deformities [35].

Rapid removal of CSF by shunt leads to a rapid decrease in the volume of the ventricular system and deformation of the cerebral cloak, as a result of the resulting pressure gradient, and additional fluid accumulations (CSF or blood) form around the brain. In some cases, acute intracranial hypotension can lead to dislocation of the brain stem and the development of vital disorders [15, 34].

The most common manifestation of this pathological condition is characterized in modern literature as “slit ventricular syndrome.”

8.2.1 The syndrome of slit ventricles of the brain

The term “slit ventricular syndrome” is widely used to describe the condition of chronic or transient headaches suffered by patients with hydrocephalus after CSF bypass operations accompanied by narrow (slit) ventricles (**Figure 9**).

There are several main pathophysiological mechanisms that cause slit ventricular syndrome: transient shunt dysfunction, intracranial hypotension, and against this background, a paroxysmal increase in ICP in the presence of a functioning shunt. At the same time, it is very important to distinguish situations when the ventricles are smaller than usual, or even almost invisible, but the clinical picture is asymptomatic and hence surgical correction is not required. Only when, in the presence of slit ventricles detected by CT/MRI examination, patients begin to suffer from an intense headache that interferes with normal life, and the diagnosis of “slit ventricular syndrome” is valid, requiring observation and treatment [36, 37].

Rekate H. suggests limiting the use of the term “slit ventricular syndrome” to cases characterized by a triad of signs: intermittent headache lasting 10–30 minutes, smaller than the normal size of the brain ventricles according to neuroimaging, slow filling of the pump reservoir after its mechanical pressure [37].

Headaches, hypodynamia, and general cerebral symptoms in these patients may be caused by both transient ICH and hypotension, and the relative significance of these mechanisms in each case seems difficult to determine.

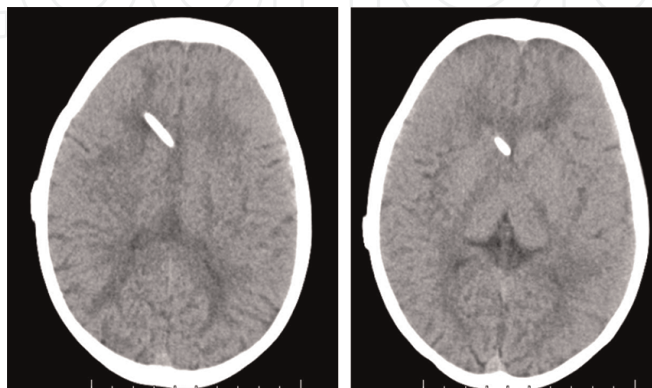


Figure 9. CT scan, axial projection of the brain 20 years after ventriculoperitoneostomy. Congenital communicating hydrocephalus. Lateral ventricles are not traced, narrow subarachnoid slits, thickened skull bones with an enhanced pattern of finger depressions.

To accurately verify the diagnosis of slit ventricular syndrome, a comprehensive examination is required, including monitoring of intracranial pressure, which will help to exclude other causes of cephalgia, for example, cases of “childhood migraine”, that is, not requiring surgical manipulations [37].

The frequency of this condition ranges from 0.9–37%, depending on the analyzed group of patients [36].

There are several pathogenetic mechanisms described in the literature and characteristic of the formation of this syndrome, underlying clinical manifestations: a sharp fluctuation of liquor pressure, deformation of liquor-containing cavities, changes in cerebrovascular conjugation, deformation of vascular collectors and redistribution of blood flow, changes in the viscoelastic properties of CSF, changes in the parameters of the regulatory mechanism implementation.

At the initial stage of the development of the slit ventricular syndrome, there is an inadequately intense CSF outflow through the shunting system, a hypotensive state, which actually leads to an excessive reduction in the size of the ventricular system. Further on, periventricular fibrosis, transient occlusion of the ventricular catheter, a decrease in the malleability of the brain, violations of venous outflow, increased intracranial pressure, etc. become the leading factors.

Neuroimaging methods are crucial in the diagnosis of slit ventricular syndrome, establishing the fact of microventriculia [37] (**Figure 10**).

Hyperdrainage syndrome requires replacement of the CSF bypass system with higher valve opening pressure values, implantation of an anti-siphon system. With narrow but asymmetric lateral ventricles, additional drainage of the opposite lateral ventricle, endoscopic perforation of the transparent septum is also proposed.

In case of confirmed dysfunction of the CSF system, it is revised with the replacement of occluded parts of the system. It is recommended to combine the revision of the liquor bypass system with the installation of an anti-siphon system, as well as during the primary implantation of the liquor bypass system, and this component should be used, which, in their opinion, prevents the development of slit ventricular syndrome [38].

In case of already formed craniostenosis with hyperdrainage in the background, when minimally invasive interventions are ineffective, when transient cephalgia persists while the shunt is functioning, and decompressive craniotomy or correction of

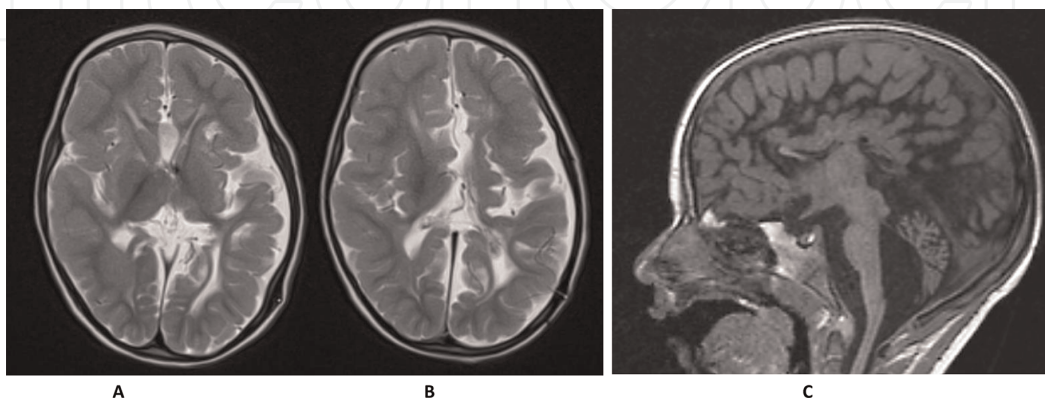


Figure 10. MRI scan of the brain 9 months after CSF bypass surgery by a low pressure valve. Posthemorrhagic hydrocephalus. Expansion of the cavity of the IV ventricle against the background of slit-like lateral and III ventricles. A, B—T2WI, axial projection; C—T1WI, sagittal projection.

cranosynostosis is recommended. According to the authors, an increase in the volume of the cranial box, in this category of children, in most cases leads to a persistent positive effect and significantly reduces the frequency of repeated revisions of the CSF system [39].

Treatment of slit ventricular syndrome should be aimed at correcting the main mechanisms of this condition development, namely, the cessation of excessive CSF outflow through the CSF bypass system, correction of cranosynostosis, microcrania, and deformation of venous collectors through craniofacial or cranial reconstructive operations [33].

8.2.2 Isolated IV ventricle syndrome

One of the specific complications of cerebrospinal bypass surgery, in particular, as a manifestation of hyperdrainage, is the “sequesterization” of various parts of the ventricular system as a result of occlusion of interventricular openings (Monroe), Monroe openings in combination with brain plumbing, brain plumbing in combination with IV ventricular openings—isolated IV ventricular syndrome.

As a result of the closure of the plumbing of the brain and the openings of the IV ventricle (Lyushka and Majendi), its isolation from the CSF system occurs. With CSF continually produced, there is a gradual expansion of the cavity of the IV ventricle and compression of adjacent structures (brain stem, cerebellum), accompanied by appropriate clinical manifestations.

This variant is rare and this pathological condition in most cases is considered as a consequence of a hyper-drainage condition. The manifestation of the isolated IV ventricle syndrome consists in cerebellar disorders and signs of stem dysfunction. More often, patients complain of impaired coordination, double vision, headache, vomiting. The progression of the pathological process often leads to an increase in bulbar symptoms, impaired consciousness, and up to coma as a result of stem structure compression [14].

The introsopic picture in isolated IV ventricle syndrome has a specific character: A significantly expanded spherical IV ventricle is visualized, squeezing the stem structures anteriorly, the cerebellum posteriorly, the bottom of the rhomboid fossa being flattened, and dislocated anteriorly. With a pronounced and prolonged nature of the pathological process, there is a caudal displacement of the amygdala of the cerebellum and rostral dislocation in the tentorial tenderloin. Other manifestations of the hyperdrainage state of the supratentorial ventricles of the brain are also typical: dilation of subarachnoid spaces, narrow or slit-shaped lateral ventricles, subdural hydromes, or hematomas of the cerebral hemispheres [40].

Isolation of the IV ventricular cavity from the CSF system is clarified by contrast examination methods (CT-ventriculography). The pathogenesis of the formation of an isolated IV ventricle can be presented in several variants (**Figure 11**).

Correction of functional occlusion of the brain's plumbing is achieved by restoring adequate control over hydrocephalus (correction of hyperdrainage state). On the other hand, a positive result in the treatment of functional occlusion of the aqueduct and thereby regression of the isolated IV ventricle syndrome can be achieved after its temporary drainage by regular punctures or implantation of the Omayya reservoir (an undesirable option) [40].

Elimination of the pressure gradient between the supra- and subtentorial spaces makes it possible to restore the participation of the IV ventricle in the CSF circulation in the functional form of this syndrome.

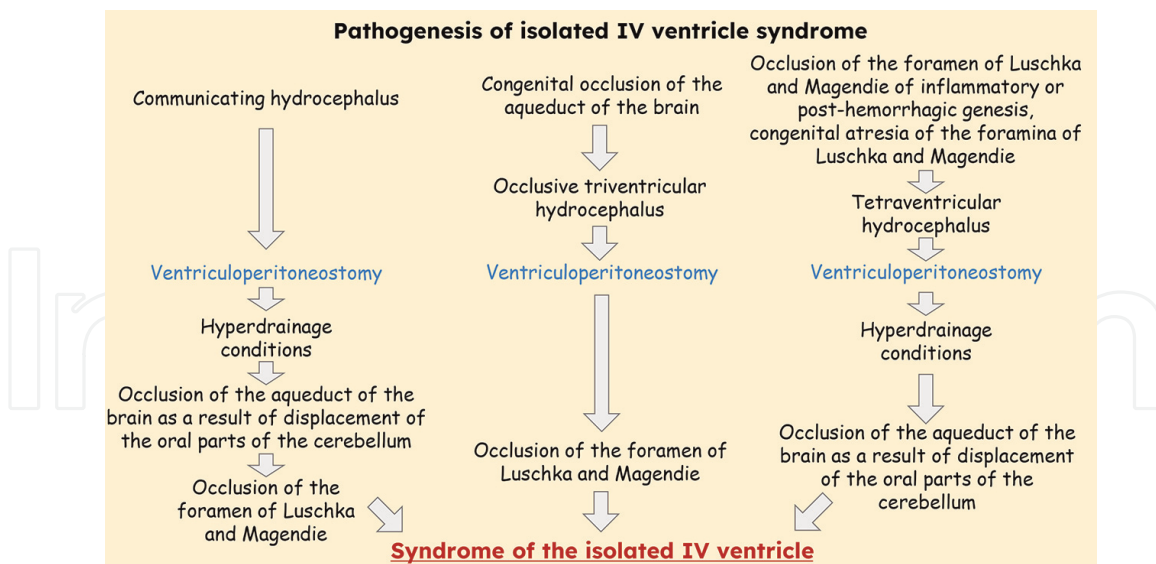


Figure 11.

Ways of formation of an isolated IV ventricle in patients with hydrocephalus after CSF bypass surgery.

In case of occlusion of the brain plumbing caused by morphological changes, surgical treatment is indicated. A number of authors practice open interventions with an isolated IV ventricle, performing microsurgical excision of adhesions, membranes causing the closure of the lumen of the brain plumbing, and ventricular openings, thus eliminating the “isolation” of the IV ventricular cavity and restoring liquor circulation by forming ventriculocysternostomy. At the same time, Dollo C. et al. recommend in some cases to complete the operation with “internal” shunting: implantation of a catheter from the cavity of the IV ventricle into the subarachnoid spinal space. The advantage of this method, according to the authors, is the prevention of re-overgrowth of the formed holes, the absence of a valve, and the position of the catheter along the rhomboid fossa bottom, which excludes damage to the latter [41].

IV ventricular bypass surgery has long been the most common method of surgical correction of the syndrome. It is worth noting that the course of the ventricular catheter should be as parallel as possible to the bottom of the rhomboid fossa, and its fixation should be reliable in order to avoid its migration into the cavity of the IV ventricle and traumatizing its bottom. When implanting a ventricular catheter, it is necessary to avoid damage to the transverse, sigmoid, and occipital sinuses [33].

A ventricular catheter is implanted through the hemispheres or, more rarely, the cerebellar worm [35] (**Figure 12, A, B**). The disadvantage of this method, according to some authors, is the impossibility of installing a ventricular catheter strictly parallel to the rhomboid fossa bottom, which does not exclude damage to the latter during surgery or when moving the brain stem against the background of ventricular drainage. With a decrease in the drainage cavity in volume, the risk of the ventricular catheter exit openings being obturated increases, which is also characteristic of this access [14].

The technique of shunting the IV ventricle through the frontal transventricular access can be described as follows: With the help of endoscopic assistance, a proximal catheter is passed through the lateral, III ventricles and installed into the cavity of the IV ventricle through the occluded water supply of the brain [42].

With this operation, simultaneous drainage of the lateral ventricles is possible with the formation of additional holes on the corresponding segments of the proximal

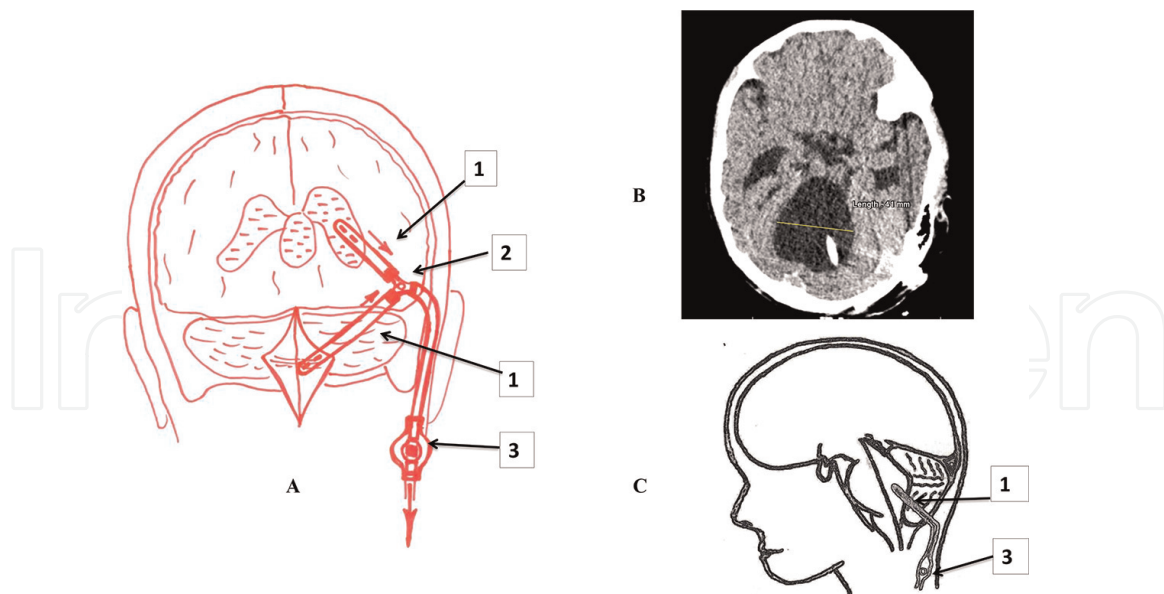


Figure 12. Isolated IV ventricle syndrome. A—Ventricular ventricular IV ventricular peritoneostomy scheme; B—CT scan, axial projection of the brain after CSF bypass surgery with IV ventricular cavity catheterization; C—IV ventricular catheterization scheme. 1—Ventricular catheter; 2—Y-shaped connector; 3—Valve.

catheter, which will allow, if necessary, to avoid implantation of additional CSF bypass systems [14].

Unfortunately, this method is not feasible in the case of narrow or slit-shaped lateral ventricles, which is often characteristic of isolated IV ventricle syndrome.

The most adequate and pathophysiologically justified method, namely, peritoneostomy through the Y-shaped system, should still be considered, in which the IV and lateral ventricles are drained by a single valve system after being preliminarily connected (ventricular-ventricular IV ventricle). The technique of the operation has already been developed. The lateral and IV ventricles are catheterized, after which the extracerebral ends of both catheters are connected by a Y-shaped system, and the third arm of the connector is connected to the valve. Next, the distal catheter is implanted in the peritoneal cavity in the usual way. This is how uniform drainage of these isolated cerebrospinal cavities is carried out (**Figure 12, C**).

After implantation, the proximal catheter is included in the general cerebrospinal bypass system through a Y-shaped connector, or separate CSF bypass systems is implanted. At the same time, according to a number of authors, preference should be given to the first option, since this allows balancing the pressure above and below the tentorium [13, 32].

At the present stage, endoscopic methods of treatment of isolated IV ventricle syndrome are most popular: aqueductoplasty with or without stenting, perforation of the bottom of the III ventricle, and restoration of patency of the holes of Lyushka and Majendi [15]. However, due to the high risk of perioperative complications (bleeding, damage to vital structures), these manipulations are recommended to be carried out only in highly qualified medical institutions.

8.3 General complications of LSO

All CSF shunting operations create artificial homeostasis, which is characterized by depressurization of the CSS, constant removal of CSF into the extracranial cavities,

prolonged implantation into the CSF system and other body cavities of a foreign body (drainage system), and fixation of intracranial pressure at a predetermined level. Under these conditions, objective prerequisites are created for the development of complications both during surgery and in the postoperative period [43, 44].

8.3.1 Complication of punctures

Puncturing of the ventricles of the brain when the proximal shunt is inserted into them can be complicated by hemorrhages into the brain tissue along the puncture channel, subdural, and intraventricular hematomas [44, 45]. In some cases, when the shunt is standing for a long time, a gliomesodermal scar forms in the surrounding brain matter. According to various authors, from 5 to 48% of liquor bypass operations are complicated by the development of epilepsy [45]. Such a large spread of data is probably explained by different ways of performing operations by different authors. For example, the risk of epilepsy development increases significantly when a shunt is performed through the frontal or temporal lobes—the zones where epileptogenic foci are most often formed. Patients who have had at least a single convulsive attack in their anamnesis or who showed high convulsive readiness during EEG examination require special attention when performing LSO.

8.3.2 Inflammatory complications

Depressurization of the cranial cavity and prolonged implantation into the ventricular shunt system creates conditions for inflammatory complications [15, 46, 47]. In 3–17% of cases, there are limited or diffuse ventriculitis, meningitis, and encephalitis of varying severity [15, 46, 47]. In these cases, it is possible to spread the infection through the shunt and the occurrence of limited or diffuse peritonitis in this regard (with ventriculoperitoneostomy). With ventriculoatriostomy, the infectious agent gets directly into the blood, which sometimes leads to the development of sepsis [15, 41]. The greatest number of inflammatory complications develops in patients operated by underqualified neurosurgeons, as well as in emaciated patients and in the absence of drug prevention [44].

8.3.3 Thromboembolic complications

The imposition of ventriculovenous anastomoses is accompanied with the introduction of a foreign body directly into the bloodstream, which can lead to thrombosis in the lumen of the sinuses, veins, or right atrium [15, 44]. Blood clots cause either vascular occlusion or serve as a source of thromboembolism of the vessels of the small circle. The death of patients in this case may occur due to reflex cardiac arrest with thromboembolism of the main vessels. Closure of the lumen of the intrapulmonary vessels can lead to the development of lung infarcts and infarct-pneumonia. Our data include a case of jugular vein thrombosis and a case a pulmonary embolism of the branches of the pulmonary artery.

8.3.4 Perineal cyst

This complication occurs when the CSF is excreted into the abdominal cavity. In the abdominal cavity, a yellowish liquid rich in protein accumulates locally around the

peritoneal end of the catheter, around which a connective tissue capsule is formed as a result of the adhesive process, without any lining [15, 43, 48].

8.3.5 *Tumor metastasis by shunt*

Before cerebrospinal bypass surgery became a regular practice, extracranial metastasis of intracranial and especially glial tumors, even with a pronounced degree of anaplasia, used to be extremely rare, which, apparently, is associated with the protective function of the blood-brain barrier [49]. The artificial CSF pathway greatly facilitates the metastasis of the tumor beyond the skull, bypassing the blood-brain barrier. Depending on the type of bypass surgery, metastatic tumors may occur in the abdominal cavity (peritoneal location of the catheter) or in the lungs (with ventriculoatriostomy) [50]. We observed metastasis of a malignant glial tumor (medulloblastoma) [44]. The primary node was located in the cerebellum, and there were multiple cerebrospinal metastases to the brain and spinal cord. Tumor tissue growths similar to the primary node were also found around the distal part of the catheter located in the retroperitoneal tissue.

8.3.6 *Violations of water-electrolyte metabolism*

The development of water-electrolyte metabolism disorders is most likely during ventriculoatriostomy, since with this type of bypass a significant and incalculable amount of CSF is removed directly into the bloodstream for a short period of time. The protein content in the liquor is 0.3 g / l, and in the blood plasma 65–85 g/l; thus, almost protein-free liquid is poured directly into the blood, which can lead to the development of hemodilution. In case this risk is ignored, the signs of hemodilution—a decrease in the number of red blood cells, hemoglobin content, protein, can be regarded as post-hemorrhagic anemia, which in turn leads to improper treatment—transfusion of a large amount of fluid [32]. In one of our observations, the child is 10 months old. During the operation, 500 ml of protein-free solutions were poured during the anesthetic aid. Immediately after the operation, a picture of stagnation in the small circle of blood circulation developed (tachypnea, diffuse wet wheezing in both lungs, tachycardia, an increase in central venous pressure), anemia, microcirculation disorders (marbled color, increased turgor, and moisture of the skin), and stem symptoms. The patient's condition was regarded as dyscirculatory (hemic) hypoxia as a result of blood loss during surgery. Blood and blood-substituting fluids (250 ml of blood and 900 ml of other solutions) were transfused, but the patient's condition continued to deteriorate, and central respiratory and hemodynamic disorders joined, resulting in death of the patient 18 hours after the operation. The cause of death of the patient in such cases is pronounced hyperhydration and hemodilution [44].

8.4 **Causes of death after CSF bypass surgery**

The death of patients after LSO most often occurs due to the progression of the underlying disease. For example, the recurrence of the tumor can cause death of cancer patients. In some cases, the complications listed above (subdural and intraventricular hematomas of large volume, brain collapse, or pronounced disorders of water-electrolyte metabolism) can be the cause of death [44]. In some cases, the death of patients (usually infants) with severe occlusive hydrocephalus occurs in the coming hours after surgery. At the autopsy, no serious complications of LSO are detected. It can

be assumed that the death of patients who were in a subcompensated state with coordinating systems of homeostasis damaged before the operation occurs due to central respiratory disorders and the activity of the cardiovascular system [32]. These disorders are probably associated with decompensation of brain stem structures. In patients with severe hydrocephalus, there is a prolonged dislocation of the trunk, to which the patient adapts. During surgery, part of the CSF is usually released into the external environment during ventriculopuncture, especially in patients with very high CSF pressure. Then, the CSF enters the extracranial cavities through the pump, due to which the CSF and intracranial pressure decrease and the brain stem is being redislocated; the pressure of the CSF on the trunk from the IV ventricle also decreases. This can probably explain increased blood filling of the brain stem present in such patients, up to the occurrence of small perivascular diapedetic hemorrhages, detected by microscopic examination. It can be assumed that in such severe patients, even minor additional damage to the trunk is sufficient for decompensation of its function and death of the patient.

9. Prospects for the use of LSO

The prospective research should be aimed at studying subtle mechanisms of CSF resorption in order to identify the possibilities of its prosthetics in case of impaired CSF circulation and hydrocephalus development. It is necessary to determine the role of lymphatic vessels and the glymphatic system in the outflow of CSF, as well as to assess the importance of vascular plexuses as the only sources of CSF production, which is questionable.

Informative criteria determining the perspective of the method of treatment of children with hydrocephalus are histobiological and anatomical-topographic features of the root cause of the disease, the presence and level of ventricular-subarachnoid dissociation, the severity of deformation of the cerebrospinal cavities, resistance to resorption of CSF, morphometric features of intracranial fluid-containing cavities, the pressure-volume index of the ratio of the CSS, and brain compliance.

In our opinion, it is promising to study the tissue characteristics of the periventricular white matter of the brain in communicating and occlusive hydrocephalus by diffusion MRI, with a quantitative assessment of the measured diffusion coefficient (ICD) and fractional anisotropy (FA) [37]. The choice of rational tactics for the treatment of children with hydrocephalus, first of all, implies taking into account and personifying these specific features of the disease manifestation (**Figure 13**).

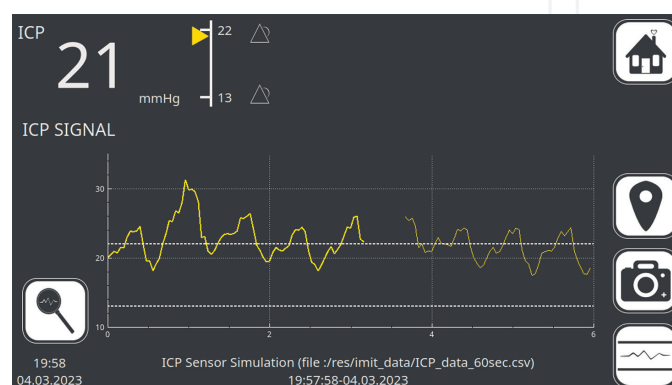


Figure 13.
High-tech instrument for analyzing intracranial pressure data.

Conducting CSF shunting operations with the selection of shunting systems require more accurate automated support, as well as digital processing and monitoring of intracranial pressure data. Modern software capabilities can allow for pressure monitoring, compliance calculation, graphical representation of pressure changes over time, external data export, etc. [51].

Improving software methods will reduce the risk of unsatisfactory results of hydrocephalus treatment by optimizing the selection of valve throughput parameters.

Thus, in the absence of currently alternative methods of surgical treatment of aresorptive hydrocephalus, it is necessary to further improve fluid shunting systems valves so that to make them capable of adapting to changing parameters of fluid circulation, including the principle of feedback.

10. Conclusions

It should be recognized that currently, the only effective and nonalternative method of treating aresorptive hydrocephalus is liquor bypass surgery. Performing LSO remains a priority mode of correcting hydrocephalus when etiotropic correction of the disease turns out to be impossible. To identify the individual features of the pathogenesis and severity of hydrocephalus, not only impaired CSF circulation, deformation of the cerebrospinal cavities and brain, but also a change in the biomechanical properties of the CSS, and evaluation of craniocerebral disproportion are significant. These mechanisms are mutually burdening each other, and their priority is variable and may change during the course of the disease, the treatment of hydrocephalus including.

The existing methods of diagnosing hydrocephalus in children based on quantitative indicators of biomechanical properties of CSF, parameters of CSF circulation, and craniocerebral ratio are sufficiently developed and informative. Strong relationship established between pulse fluctuations of intracranial pressure, brain compliance, “pressure-volume” ratio of CSF, and CSF circulation is of

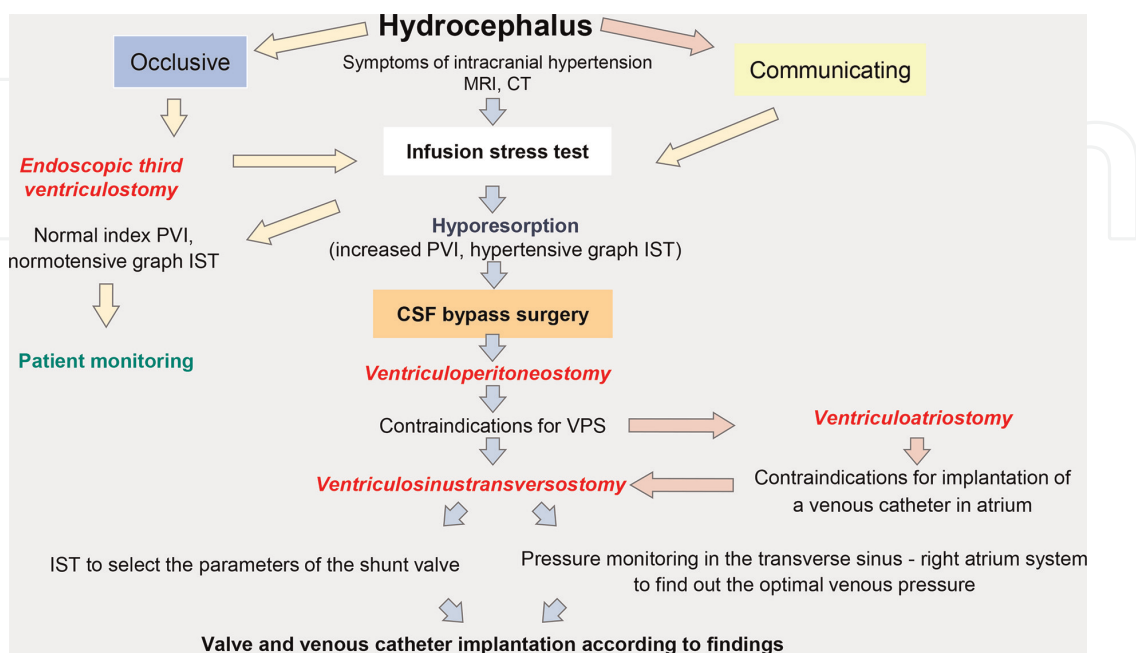


Figure 14.
 Tactics for the treatment of hydrocephalus.

diagnostic significance. Evaluation of pulse fluctuations of intracranial volume allows minimally invasive personalized quantification of the parameters of CSF circulation and biomechanical properties of the CSS and craniocerebral ratio (**Figure 14**).

When choosing a treatment method, preference is given to pathogenetic interventions. The leading diagnostic method for hydrocephalus is a quantitative assessment of hydrocephalus, parameters of CSF circulation, and biomechanical properties of CSF (PVI, compliance, cerebrospinal pressure curve).

Evaluation of CSF circulation parameters and the CSS compliance requires modern hardware. In this regard, new evaluation methods are currently being developed and the existing ones are being improved to make the study accurate, minimally invasive, and informative.

Acknowledgements

We thank the neurosurgeons and neurologists of the Polenov Institute involved in the treatment of hydrocephalus in child patients who helped in the creation of this chapter.

The work was supported by the state task of the National Almazov Medical Research Center No. 121031100314-1.

Conflict of interest

The authors declare no conflict of interest.

Appendices and nomenclature

CNS	central nervous system
CSF	cerebrospinal fluid
CSS	craniospinal system
ETV	endoscopic third ventriculostomy
ICH	intracranial hypertension
LS	liquor shunting operations
NTDFS	folate-sensitive neural tube defects
MPPH	Megalencephaly-polymicrogyria-polydactyly-hydrocephalus syndrome
ICC	intracranial compliance
IST	infusion stress test
MRI	magnetic resonance imaging
MSCT	magnetic spiral computed tomography
PVI	pressure volume index
VSTS	ventriculosinuversostomy

IntechOpen

Author details

Konstantin A. Samochernykh¹, Yulia M. Zabrodskaia^{1*}, Mikhail S. Nikolaenko¹, Olga N. Gaykova², Aleksandr V. Kim¹, Elena G. Potemkina¹, Aleksandr P. Gerasimov¹, Nikita K. Samochernykh¹, Aleksey A. Petukhov³, Eleonora T. Nazaralieva⁴ and Wiliam A. Khachatryan¹

1 Polenov Russian Scientific Research Institute of Neurosurgery – Branch of Almazov National Medical Research Centre of Ministry of Health of Russian Federation, Saint-Petersburg, Russia


2 Golikov Research Center of Toxicology, Saint-Petersburg, Russia

3 Limited Liability Company “SIC Radio Engineering”, Saint-Petersburg, Russia

4 Department of Paediatric Neurosurgery, Almazov National Medical Research Centre of Ministry of Health Care of Russian Federation, Saint Petersburg, Russian Federation

*Address all correspondence to: zabrjulia@yandex.ru

IntechOpen

© 2023 The Author(s). Licensee IntechOpen. This chapter is distributed under the terms of the Creative Commons Attribution License (<http://creativecommons.org/licenses/by/3.0>), which permits unrestricted use, distribution, and reproduction in any medium, provided the original work is properly cited. 

References

- [1] Arend AA. Hydrocephalus and its Surgical Treatment. Moscow: Medicine; 1948. p. 200 (In Russ.)
- [2] Garmashov YuA, Iova AS, Iova DA, et al. Perinatal Neurosurgery. Fundamentals of Optimal Medical Care. St. Petersburg. 2015. –156 p. (In Russ.)
- [3] Khachatryan WA, Samochernykh KA, Kim AV, Nikolaenko MS, Sysoev KV, Don OA, et al. Ventriculo-sinus-transversal shunt in the treatment of decompensated hydrocephalus in children (the results of clinical testing of the method). Translational Medicine. 2017;4(1):20-28. (In Russ.). DOI: 10.18705/2311-4495-2017-4-1-20-28
- [4] Padayachy L, Ford L, Dlamini N, Mazwi A. Surgical treatment of post-infectious hydrocephalus in infants. Child's Nervous System. 2021;37(11):3397-3406. DOI: 10.1007/s00381-021-05237-1 Epub 2021 Jun 19
- [5] Yengo-Kahn AM, Wellons JC, Hankinson TC, Hauptman JS, Jackson EM, Jensen H, et al. Hydrocephalus clinical research network. Treatment strategies for hydrocephalus related to Dandy-Walker syndrome: Evaluating procedure selection and success within the hydrocephalus clinical research network. Journal of Neurosurgery. Pediatrics. 2021:1-9. DOI: 10.3171/2020.11.PEDS20806 [Epub ahead of print]
- [6] Tully HM, Dobyens WB. Infantile hydrocephalus: A review of epidemiology, classification and causes. European Journal of Medical Genetics. 2014;57(8):359-368. DOI: 10.1016/j.ejmg.2014.06.002 Epub 2014 Jun 13
- [7] Wu Q, Sun L, Xu Y, Yang X, Sun S, Wang W. Diagnosis of a fetus with X-linked hydrocephalus due to mutation of L1CAM gene. Zhonghua Yi Xue Yi Chuan Xue Za Zhi. 2019;36(9):897-900. Chinese. DOI: 10.3760/cma.j.issn.1003-9406.2019.09.011
- [8] Muir RT, Wang S, Warf BC. Global surgery for pediatric hydrocephalus in the developing world: A review of the history, challenges, and future directions. Neurosurgical Focus. 2016;41(5):E11. DOI: 10.3171/2016.7.FOCUS16273
- [9] Miyajima M, Arai H. Evaluation of the production and absorption of cerebrospinal fluid. Neurologia Medico-Chirurgica. 2015;55(8):647-656
- [10] Filis AK, Aghayev K, Vrionis FD. Cerebrospinal fluid and hydrocephalus: Physiology, diagnosis, and treatment. Cancer Control. 2017;24(1):6-8. DOI: 10.1177/107327481702400102
- [11] Jeng S, Gupta N, Wrensch M, Zhao S, Wu YW. Prevalence of congenital hydrocephalus in California, 1991-2000. Pediatric Neurology. 2011;45(2):67-71. DOI: 10.1016/j.pediatrneurol.2011.03.009
- [12] Khachatryan WA, Samochernykh KA. Endoscopy in Pediatric Neurosurgery. Branco, Saint-Petersburg. 2015. p. 276 (In Russ.)
- [13] Kommunarov VV, Khachatryan WA, Chmutin GE, Gogoryan SF. Selection of parameters of the CSF shunting system in the treatment of hydrocephalus. Scientific and Practical. and. Neurosurgery and Neurology of Childhood. 2005;3:72-84 (In Russ.)

- [14] Rekate HL. Classification of slit-ventricle syndromes using intracranial pressure monitoring. *Pediatric Neurosurgery*. 1993;**19**(1):15-20. DOI: 10.1159/000120694
- [15] Atiskov YA, Riznich VP, Khachatryan WA. A craniospinal compliance monitor. *Biomedical Engineering*. 2021;**54**(6):380-383
- [16] Riva-Cambrin J, Kestle JR, Holubkov R, Butler J, Kulkarni AV, Drake J, et al. Hydrocephalus clinical research network. Risk factors for shunt malfunction in pediatric hydrocephalus: A multicenter prospective cohort study. *Journal of Neurosurgery. Pediatrics*. 2016;**17**(4):382-390. DOI: 10.3171/2015.6.PEDS14670 Epub 2015 Dec 4
- [17] Varagur K, Sanka SA, Strahle JM. Syndromic hydrocephalus. *Neurosurgery Clinics of North America*. 2022;**33**(1):67-79. DOI: 10.1016/j.nec.2021.09.006
- [18] Massimi L, Paternoster G, Fasano T, Di Rocco C. On the changing epidemiology of hydrocephalus. *Child's Nervous System*. 2009;**25**(7):795-800. DOI: 10.1007/s00381-009-0844-4 Epub 2009 Feb 24
- [19] Iourov IY, Gerasimov AP, Zelenova MA, Ivanova NE, Kurinnaia OS, Zabrodskaya YM, et al. Cytogenomic epileptology. *Molecular Cytogenetics*. 2023;**16**(1):1. DOI: 10.1186/s13039-022-00634-w
- [20] Lei Y, Zhu H, Yang W, Ross ME, Shaw GM, Finnell RH. Identification of novel CELSR1 mutations in spina bifida. *PLoS One*. 2014;**9**(3):e92207. DOI: 10.1371/journal.pone.0092207
- [21] Kibar Z, Torban E, McDearmid JR, Reynolds A, Berghout J, Mathieu M, et al. Mutations in VANGL1 associated with neural-tube defects. *The New England Journal of Medicine*. 2007; **356**(14):1432-1437. DOI: 10.1056/NEJMoa060651
- [22] Detrait ER, George TM, Etchevers HC, Gilbert JR, Vekemans M, Speer MC. Human neural tube defects: Developmental biology, epidemiology, and genetics. *Neurotoxicology and Teratology*. 2005;**27**(3):515-524. DOI: 10.1016/j.ntt.2004.12.007 Epub 2005 Mar 5
- [23] Bott L, Boute O, Mention K, Vinchon M, Boman F, Gottrand F. Congenital idiopathic intestinal pseudo-obstruction and hydrocephalus with stenosis of the aqueduct of sylvius. *American Journal of Medical Genetics. Part A*. 2004;**130A**(1):84-87. DOI: 10.1002/ajmg.a.30793
- [24] Rivière JB, Mirzaa GM, O'Roak BJ, Beddaoui M, Alcantara D, Conway RL, et al. De novo germline and postzygotic mutations in AKT3, PIK3R2 and PIK3CA cause a spectrum of related megalencephaly syndromes. *Nature Genetics*. 2012;**44**(8):934-940. DOI: 10.1038/ng.2331
- [25] Larrew TW, Eskandari R. Pediatric hydrocephalus: Current state of diagnosis and treatment. *Pediatrics in Review*. 2016;**37**(11):478-490
- [26] Vlasov EA. Tomographic (CT and MRI) Anatomy of the Human Central Nervous System. Atlas. Moscow: Vidar-M Publishing House; 2020. p. 144
- [27] Trofimova TN, Ananyeva NI, Nazinkina YV, Karpenko AK, Khalikov AD. *Neuroradiology*. St. Petersburg: Publishing house of St. Petersburg MAPO; 2005. p. 288
- [28] Gogorian SF, Bersnev VP, Kim AV, Samochernykh KA, Malkhosian ZhG.

Brain tumors combined with hydrocephalus. Zhurnal Voprosy Neirokhirurgii Imeni N. N. Burdenko. 2008;**82**(4):39-42; discussion 42-3. (In Russ.)

[29] Rekate HL. Hydrocephalus in infants: The unique biomechanics and why they matter. Child's Nervous System. 2020;**36**(8):1713-1728. DOI: 10.1007/s00381-020-04683-7 Epub 2020 Jun 2

[30] Zabrodskaya YM, Medvedev YA, Sukhatskaya AV, Trofimova TN, Ananjeva NI. Perifocal changes of brain substance near long-existing shunts (MRI-morphological comparison). Neurology Bulletin. 2007;**39**(2):80-85 (In Russ.)

[31] Albright AL. Hydrocephalus shunt practice of experienced pediatric neurosurgeons. Child's Nervous System. 2010;**26**(7):925-929. DOI: 10.1007/s00381-010-1082-5 Epub 2010 Feb 9

[32] Lubnin AY, Korshunov AG, Simernitsky VP. Analysis of the causes of deaths in the surgical treatment of hydrocephalus in children. Zhurnal Voprosy Neirokhirurgii Imeni N.N. Burdenko. 1993;**2**:26-29 (In Russ.)

[33] Benzel EC, Reeves JD, Kesterson L, Hadden TA. Slit ventricle syndrome in children: Clinical presentation and treatment. Acta Neurochirurgica. 1992;**117**(1-2):7-14. DOI: 10.1007/BF01400628

[34] McAllister JP 2nd. Pathophysiology of congenital and neonatal hydrocephalus. Seminars in Fetal and Neonatal Medicine. Oct 2012;**17**(5):285-294. DOI: 10.1016/j.siny.2012.06.004. Epub 2012 Jul 15. PMID: 22800608

[35] Allan R, Chaseling R. Subtemporal decompression for slit-ventricle

syndrome: Successful outcome after dramatic change in intracranial pressure wave morphology. Report of two cases. Journal of Neurosurgery. 2004;**101**(2 Suppl):214-217. DOI: 10.3171/ped.2004.101.2.0214

[36] Colpan ME, Savas A, Egemen N, Kanpolat Y. Stereotactically-guided fourth ventriculo-peritoneal shunting for the isolated fourth ventricle. Minimally Invasive Neurosurgery. 2003;**46**(1):57-60. DOI: 10.1055/s-2003-37960

[37] Shevtsov MA, Senkevich KA, Kim AV, Gerasimova KA, Trofimova TN, Kataeva GV, et al. Changes of fractional anisotropy (FA) and apparent diffusion coefficient (ADC) in the model of experimental acute hydrocephalus in rabbits. Acta Neurochirurgica. 2015;**157**(4):689-698. DOI: 10.1007/s00701-014-2339-7 discussion 698. Epub 2015 Jan 16

[38] Oi S, Matsumoto S. Pathophysiology of aqueductal obstruction in isolated IV ventricle after shunting. Child's Nervous System. 1986;**2**(6):282-286. DOI: 10.1007/BF00271938

[39] Cinalli G, Spennato P, Savarese L, Ruggiero C, Aliberti F, Cuomo L, et al. Endoscopic aqueductoplasty and placement of a stent in the cerebral aqueduct in the management of isolated fourth ventricle in children. Journal of Neurosurgery. 2006;**104**(1 Suppl):21-27. DOI: 10.3171/ped.2006.104.1.21

[40] Sysoev KV, Ivanov VP, Kim AV, Samochernyh KA, Khachatryan WA. Ventricle-sinus transversostomy in treatment of hydrocephalus. Child's Nervous System. 2016;**32**:975. DOI: 10.1007/s00381-016-3044-z

[41] McGirt MJ, Zaas A, Fuchs HE, George TM, Kaye K, Sexton DJ. Risk factors for pediatric ventriculoperitoneal shunt infection and predictors of

infectious pathogens. *Clinical Infectious Diseases*. 2003;**36**(7):858-862.
DOI: 10.1086/368191 Epub 2003 Mar 18

[42] Bayston R, Grove N, Siegel J, Lawellin D, Barsham S. Prevention of hydrocephalus shunt catheter colonisation in vitro by impregnation with antimicrobials. *Journal of Neurology, Neurosurgery, and Psychiatry*. 1989;**52**(5):605-609.
DOI: 10.1136/jnnp.52.5.605

[43] Hanak BW, Bonow RH, Harris CA, Browd SR. Cerebrospinal fluid shunting complications in children. *Pediatric Neurosurgery*. 2017;**52**(6):381-400.
DOI: 10.1159/000452840 Epub 2017 Mar 2

[44] Gaykova ON, Khachatryan WA, Ryabukha NP, Zelenkova LA. Pathological anatomical diagnosis of complications of CSF shunting operations. Teaching booklet. Saint-Petersburg. 1996. p. 10 (In Russ.)

[45] Wong JM, Ziewacz JE, Ho AL, Panchmatia JR, Bader AM, Garton HJ, et al. Patterns in neurosurgical adverse events: Cerebrospinal fluid shunt surgery. *Neurosurgical Focus*. 2012;**33**(5):E13. DOI: 10.3171/2012.7.FOCUS12179

[46] Conen A, Walti LN, Merlo A, Fluckiger U, Battegay M, Trampuz A. Characteristics and treatment outcome of cerebrospinal fluid shunt-associated infections in adults: A retrospective analysis over an 11-year period. *Clinical Infectious Diseases*. 2008;**47**(1):73-82.
DOI: 10.1086/588298

[47] Crnich CJ, Safdar N, Maki DG. Infections associated with implanted medical devices. In: Finch RG, Greenwood D, Norrby SR, Whitley RJ, editors. *Antibiotic and Chemotherapy: Anti-Infective Agents and their Use in*

Therapy. 8th ed. Edinburg: Churchill Livingstone; 2003. pp. 575-618

[48] Dabdoub CB, Dabdoub CF, Chavez M, Villarroel J, Ferrufino JL, Coimbra A, et al. Abdominal cerebrospinal fluid pseudocyst: A comparative analysis between children and adults. *Child's Nervous System*. 2014;**30**(4):579-589. DOI: 10.1007/s00381-014-2370-2 Epub 2014 Jan 29

[49] Zheludkova OG, Olkhova LV. Shunt-associated extraneural metastasis of tumors central nervous system: A literature review. *Pediatricskii vestnik Juznogo Urala*. 2020;**1**:27-38. (In Russ.). DOI: 10.34710/Chel.2020.40.53.004

[50] Narayan A, Jallo G, Huisman TA. Extracranial, peritoneal seeding of primary malignant brain tumors through ventriculo-peritoneal shunts in children: Case report and review of the literature. *The Neuroradiology Journal*. 2015;**28**(5): 536-539. DOI: 10.1177/1971400915609348 Epub 2015 Oct 6

[51] Atiskov YA, Khachatryan WA, Nazarialieva ET and others. A Craniospinal compliance monitor. *Biomedical Engineering*. 2021;**54**: 380-383. DOI: 10.1007/s10527-021-10044-8